scientific reports

Check for updates

OPEN

Immune profiling identifies the contribution of extracellular vesicles to immune modulation and progression in prostate cancer

Giovanni Pecoraro[1,3], Ginevra Sarnacchiaro[1], Giovanni Smaldone[1], Andrea Soricelli[1,2] & Jessie Santoro[1,3]✉

Prostate cancer is the fourth leading cause of death in men worldwide. Currently, the gold standard for PCa diagnosis remains the Prostate-Specific Antigen (PSA); therefore, there is a growing demand for novel diagnostic approaches for early prediction of aggressive types of prostate cancer. The complexity of tumors is further enhanced by the presence of extracellular vesicles (EVs). These membrane-enclosed spherical particles are directly derived from their parent cells with their information (mRNAs, non-coding RNAs, and proteins) and play a critical role in intercellular communication. However, the role of PCa EVs in the crosstalk between cancer cells and resident cells in the microenvironment is still under investigation. Different prostate cancer cell lines were cultured for 48 h in medium supplemented with FBS exo-free medium. Next, secreted EVs were separated using differential ultracentrifugation, and further EVs characterization was performed by nanoparticle tracking analysis, immunoblotting, and scanning electron microscopy. The effect of prostate cancer EVs on the immune cell population was analyzed after staining PBMCs using flow cytometry. Additionally, cytokines released into the conditioned media were evaluated using an ELISA assay. We illustrated how EVs from prostate cancer cells of different background variously affected immune cells and modulated the expression of several cytokines after 24 h of treatment. We observed that the number of rare monocytes, CD14 + CD16 + , was significantly reduced in PBMCs treated with PC-3 and DU 145 EVs compared with LNCaP EVs. Furthermore, CD4 + and CD8 + activated cells were significantly more responsive when PBMCs were treated with PC-3 EVs compared to LNCaP EVs. Subsequently, pro- and anti-inflammatory cytokines were found to be more abundant in samples treated with PC-3 and DU 145 EVs. This suggests a potential role of EVs in prostate cancer progression and immune system evasion. Our study provides preliminary evidence that prostate cancer EVs exert distinct immunomodulatory effects, depending on their cellular origin. Ultimately, the differences observed between PC-3 EVs, DU 145 EVs and LNCaP EVs highlight the potential use of immune cell markers as reliable indicators of disease progression and as a non-invasive tool to complement prostate cancer risk stratification strategies.

Keywords Prostate cancer, Extracellular vesicles, Microenvironment, Early diagnosis, Immune cells

Prostate cancer (PCa) is the second most diagnosed neoplasia in men, with approximately 1.47 million cases worldwide and 397,000 deaths caused by the disease in 2022, accounting for approximately 7.3% of all cancers[1]. Although the highest incidence of PCa is found in Northern Europe, the mortality rate reaches a peak in Southern Africa, indicating how the importance of a developed healthcare system can affect the possibility of recovery from this disease[1]. The age distribution of the disease follows a clear pattern, with rare cases occurring under the age of 40 years and a peak after 55 years[2]. Diagnosis of prostate adenocarcinomas is mainly based on histopathological aspects, including glandular architecture, absence of basal cells, and nuclear atypia of the glandular lining cells[3]. Currently, PCa prognosis relies on the evaluation of three parameters: serum levels of Prostate-Specific Antigen (PSA), Gleason Score (GS), and Tumor Node Metastasis (TNM)[4,5]. However, risk stratification based solely on these factors still presents limitations in guiding treatment choices, and further studies are required[6]. While early-stage PCa has slow progression and can be either actively monitored or efficiently treated with radical

[1]IRCCS SYNLAB SDN, Via G. Ferraris 144, 80146 Napoli, Italy. [2]Department of Medical, Movement and Wellbeing Sciences, University of Naples Parthenope, Naples, Italy. [3]Giovanni Pecoraro and Jessie Santoro equally contributed to this work. ✉email: jessie.santoro@synlab.it

prostatectomy or external-beam radiation therapy, localized advanced PCa requires additional therapeutic approaches, including androgen deprivation therapy (ADT) and chemotherapy[6,7]. Once metastatic, PCa can be further classified based on its response to ADT into hormone-sensitive (mHSPC) or castration-resistant prostate cancer (mCRPC)[8]. Preclinical models of PCa are essential for studying cancer development and identifying viable treatment options, and established cell lines, such as LNCaP[9], DU 145[10] and PC-3[11], are still the most used models for studying the phenomena of PCa differential aggressiveness[12]and androgen sensitivity or independence[13]. While all three cell lines were derived from metastatic sites, LNCaP cells retain AR positivity and PSA expression, sensitivity to anti-androgen drugs, and show a low proliferation rate[9]. Conversely, DU 145 and PC-3 cells are AR- and PSA-negative, insensitive to ADT, and increasingly aggressive, with PC-3 being the most invasive ones[12,14] . Given this information, the three cell models cover different zones of the prostate cancer malignancy spectrum. It is becoming more evident that the tumor microenvironment (TME) plays a crucial role in regulating tumor progression and metastasis[14]. TME is defined as a complex milieu that surrounds and envelopes the tumor and is composed of different types of cells, including stromal cells, fibroblasts, endothelial cells, and innate and adaptive immune cells[15]. In the context of PCa, the immune components of the PCa microenvironment, which reside within the niche, can determine the ability of the tumor to escape the immune response and facilitate cancer cell migration toward distant sites. Moreover, PCa is represented by higher intratumoral levels of CD8 + T cells correlating with poorer outcomes and increased metastatic potential[16,17]. Similarly, the abundance of B cells in the TME correlates with increased aggressiveness[18] and facilitates the emergence of a castration-resistant profile[19] as well as in determining the immune escape of PCa cells, especially through their interaction with CD8 + T cells[20,21]. Extracellular vesicles (EVs) play a crucial role in the complex network between tumors and immune cells[22]. EVs are membrane-enclosed particles that can transfer their cargo from an originating cell to different recipient cells and modulate their function[23,24]. In the context of prostate cancer, EVs produced by cancer cells have been linked to the promotion of neo-angiogenesis and vascular leakage at both the primary tumor site and pre-metastatic niche[25–27]. Furthermore, in situ secretion of EVs by PCa cells hampers lymphocyte activity and induces CD8 + T-cell death[28]. Additionally, EVs are essential for mediating cell-to-cell communication, and prostate cancer EVs may actively participate in the mechanisms of immune escape[29,30].

In this study, we established a model to analyse the effects of PCa EVs on peripheral blood mononuclear cells (PBMCs) from healthy patients and investigated how EVs of different aggressiveness could modulate the abundance of specific immune subpopulations and cytokine production. Our work aims to shed light on the possibility of further investigating how EVs modulate immune cell populations as a predictive, non-invasive tool to complement prostate cancer risk stratification strategies and improve the definition of best-fitting therapeutic approaches for personalized medicine.

Results

Characterisation of prostate cancer EVs

The particle concentration and size of EVs separated from PC-3, LNCaP and DU 145 cells were quantified by nanoparticle tracking analysis (Fig. 1a). Specifically, the particle concentration in PC-3 EVs samples was 7×10^{10} particles/mL whereas for LNCaP EVs was 3.5×10^{10} particles/mL and for DU 145 was 5.9×10^{9}. Mean size in PC-3 EVs was 130 nm; in contrast, for LNCaP EVs and DU 145 EVs was 110 nm in diameter, as shown in the representative peaks in Fig. 1b. A single peak for each EVs was detected by NTA, which showed a homogenous population of EVs in all the samples (Fig. 1b). To confirm the presence of EVs in our samples, prostate cancer EVs were processed for western blot analysis after ultracentrifugation (Fig. 1c; Supplementary Fig. 1). Following the MISEV2023 guidelines[31] we detected two EVs-associated proteins, syntenin, CD63 and one non-EVs marker calnexin, known as an endoplasmic reticulum (ER) protein. For syntenin, clear bands were observed for PC-3, LNCaP and DU 145 EVs. Similarly, tetraspanin CD63 was detected in all prostate cancer-derived EVs; however, in PC-3 and DU 145 EVs the signal was slightly fainter than that of LNCaP EVs (Fig. 1c). As expected, the ER marker calnexin was not detected in any of the EVs samples. Accordingly, positive controls were used, and the three corresponding cell lines, were positive for all markers mentioned above, including calnexin, which confirmed the enrichment of EVs in our samples (Fig. 1c). Furthermore, EVs morphology and structure was observed using scanning electron microscopy, as shown in Fig. 1d (PC-3 EVs),1e (LNCaP EVs) and 1f. (DU 145 EVs). Overall, vesicles derived from the three cell lines cells were round and consistent with the typical EVs-like particle morphology. Moreover, the detected size of purified EVs from scanning electron microscopy ranged from 90 to 130 nm, in line with the mean size calculated by NTA (Fig. 1b).

Effect of prostate cancer EVs on monocyte populations

Monocytes are essential components of the circulating immune system and respond first to foreign stimuli. We evaluated the effects of EVs derived from prostate cancer cell lines with different degrees of aggressiveness on PMBCs derived from ten healthy donors after 6 h of EVs treatment. Gating strategy used was reported in Supplementary Fig. 2. No differences were observed in the percentages of CD14 + cells, CD16 + CD14- rare monocytes, and activated cells (see Supplementary Fig. 3). Instead, as shown in Fig. 2a, we observed a significant ($p < 0.001$) reduction in CD14 + CD16 + cells in PC-3 and DU 145-EVs treated PBMCs compared to LNCaP-EVs treated PBMCs. Interestingly, the same effect was observed by comparing the % of CD14 + CD16 + cells found in the untreated cells compared to PC-3 and DU 145-EVs treated cells (Fig. 2 b; $p < 0.001$ and $p > 0.0001$ for PC-3 and DU 145, respectively). Conversely, the % of CD14 + CD16 + cells showed no differences compared to untreated PBMCs and LNCaP-EVs treated PBMCs (Fig. 2b). To investigate whether the observed differences in the percentage of CD14 + CD16 + monocytes compared to LNCaP-EVs treated were correlated to androgen irresponsiveness of PC-3 and DU 145 cells, we also tested EVs derived from neuroendocrine transdifferentiated LNCaP (tNEPC LNCaP) cells, by cultivating parental LNCaP cells for 18 days in androgen-deprived medium.

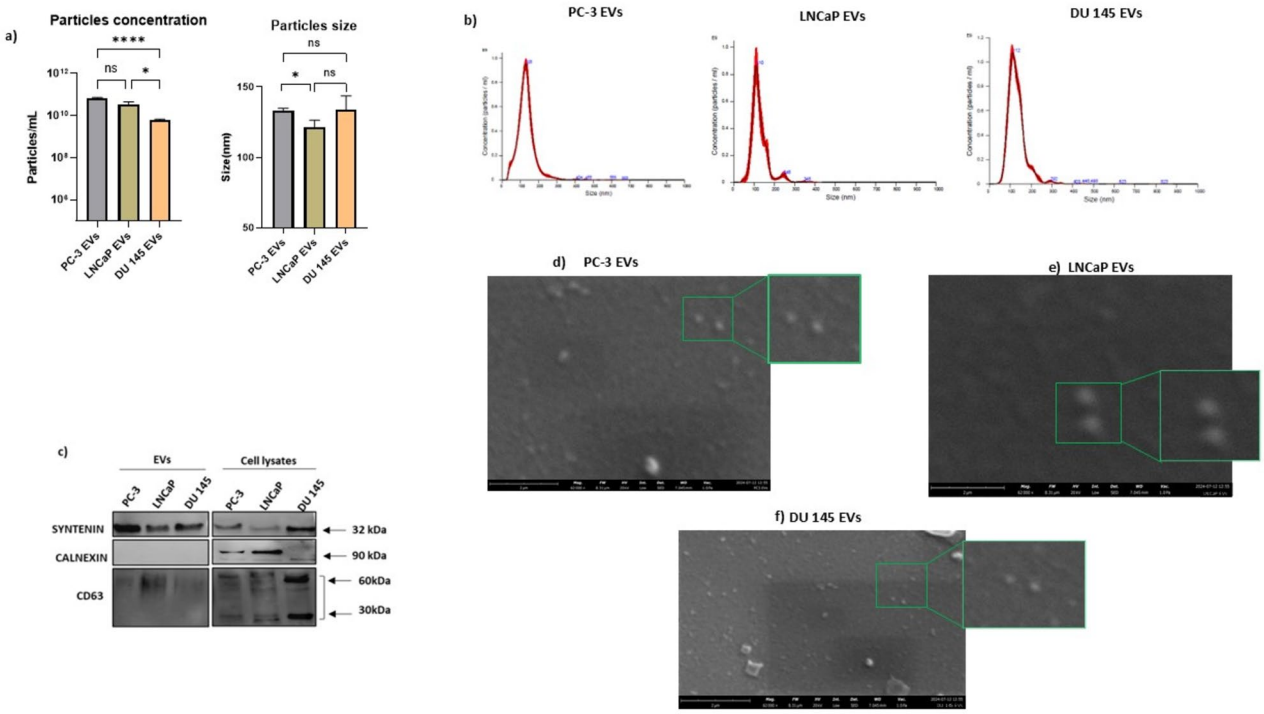

Fig. 1. Characterisation of prostate cancer-derived extracellular vesicles. EVs post differential ultracentrifugation were characterised using nanoparticle tracking analysis (NTA), immunoblotting analysis, and scanning electron microscopy (SEM). **a**). Particle concentration and size of which three replicates of each sample were analysed by NTA independently. Data analysed by one-way ANOVA test and presented as mean bars (n = 3) ± SEM, the significant p-value is reported; * indicates $p < 0.05$, ** indicates $p < 0.01$. n.s. = not significant. **b**) Representative graphs of prostate cancer EVs distribution from NTA software. **c**) Immunoblotting analysis of EVs from PC-3, LNCaP and DU 145 cells and cell lysates. Detection of EVs associated positive markers, syntenin, CD63, and negative marker calnexin. SEM images of **d**) PC-3 EVs, **e**) LNCaP EVs and f) DU 145 EVs with a range of 90 nm to 130 nm (magnification 62000x).

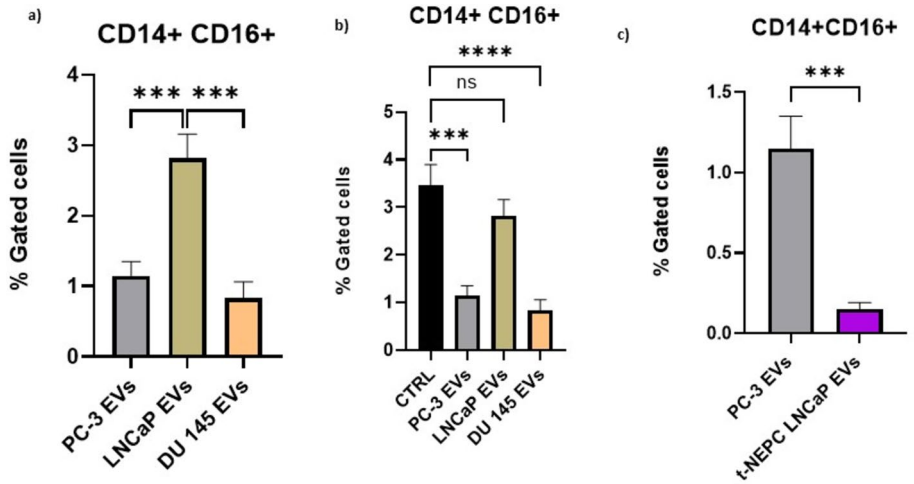

Fig. 2. Effect of PC-3 and LNCaP EVs on monocyte populations. PBMCs were treated with PC-3 EVs, LNCaP EVs, DU 145 EVs and t-NEPC LNCaP EVs for 24 h. **a**) Comparison of % CD14 + CD16 + rare monocytes from 10 healthy volunteers treated with EVs derived from PC-3, LNCaP and DU 145. **b**) Comparison of % CD14 + CD16 + rare monocytes treated with EVs derived from PC-3, LNCaP and DU 145 in respect to the untreated samples (CTRL). **c**) Comparison of % CD14 + CD16 + rare monocytes treated with EVs derived from PC-3 compared to t-NEPC LNCaP treated cells. Data analysed by one-way ANOVA and presented as mean bars (n = 10) ± SEM, the significant *p*-value is reported; **** $p < 0.0001$; *** indicates $p < 0.001$; n.s. = not significant.

Successful neuroendocrine transdifferentiation was confirmed by protein increase of neuron-specific enolase (ENO2) and chromogranin A (CHGA) (Supplementary Fig. 4a). Moreover, when exposed to tNEPC LNCaP-EVs, monocyte populations strongly decreased when compared to LNCaP EVs treated PBMCs (Supplementary Fig. 4b). Hence, comparison with PC-3-EVs treated monocytes revealed a significant ($p < 0.001$) decrease in CD14 + CD16 + cells (Fig. 2c).

PC-3-EVs have greater effects on the immune cell population compared to LNCaP-EVs

The same experiments were performed using a mix of antibodies capable of identifying innate lymphoid cells and NK cells. Gating strategy used for this analysis was reported in Supplementary Fig. 5. As shown in Supplementary Fig. 6, there were no significant differences in the percentage of CD56 + CD3 +, CD335 +, CD337 +, and CD335 + /CD337 + NK cells, nor in their ability to activate. Surprisingly, there is no significant difference between the percentage of CD4 + and CD8 + cells in the PC-3 and DU 145 EVs treated PBMCs compared to the LNCaP-EVs treated cells (Supplementary Fig. 7 and 8). On the other hand, , CD4 + HLA-DR + cells and CD8 + HLA-DR + cells were significantly ($p < 0.05$) more abundant after 24 h of treatment with EVs from PC-3 cells rather than EVs from LNCaP cells (Fig. 3a and b). This became even more relevant when we considered the ratio of activated cells to total number of cells (Fig. 3c and d). Conversely, in the case of DU 145 EVs treatment, no statically significant differences were observed for the % of CD4 + HLA-DR, CD8 + HLA-DR + cells compared to LNCaP EVs treatment (Fig. 3a and b) as well as the associated cell ratios (Fig. 3c and d). In addition, we observed no significant differences in the percentages of activated cells and cell ratios for

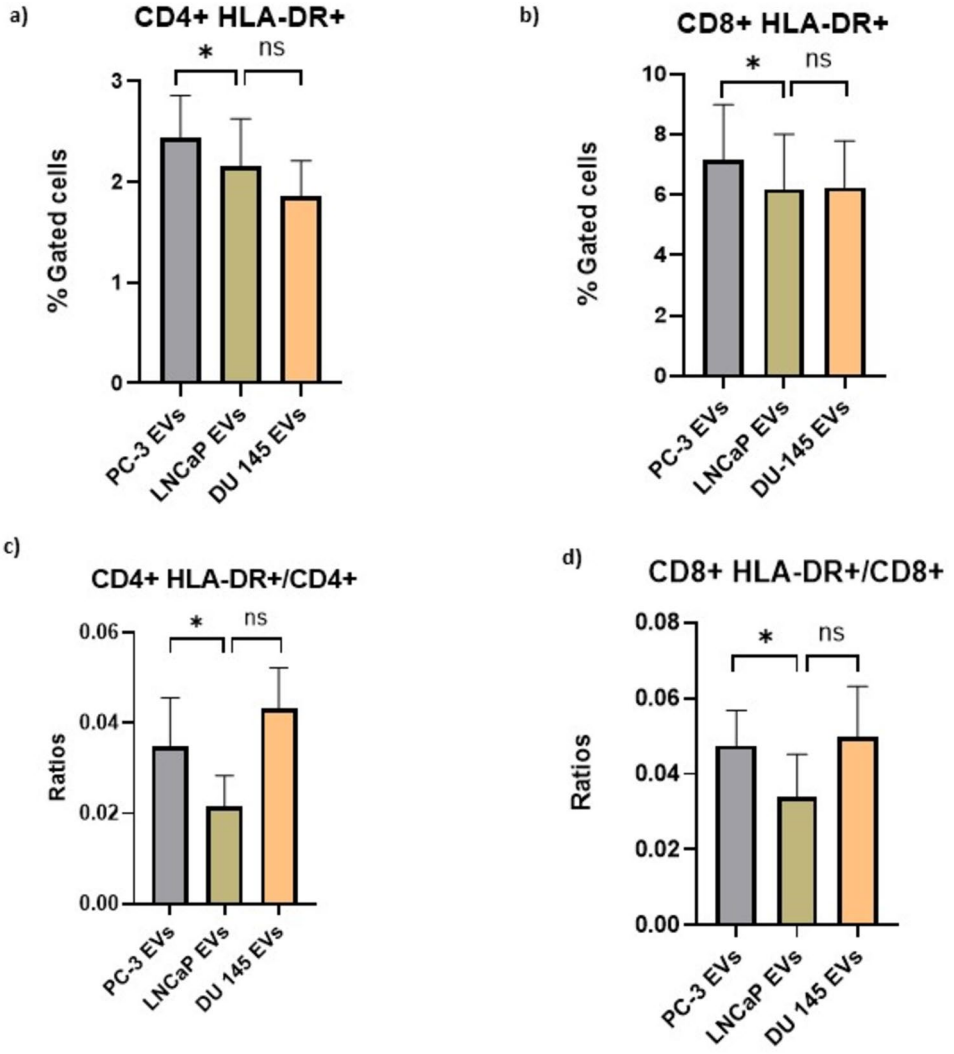

Fig. 3. PC-3-EVs effects on innate lymphoid and NK cells compared to LNCaP-EVs. Effect of prostate cancer EVs on innate immune cells. **a**) The percentage of CD4 + HLA-DR + after treatment with EVs derived from PC-3 and DU 145 compared to LNCaP treatment. **b**) The percentage of CD8 + HLA-DR + treated with EVs derived from PC-3 and DU 145 in comparison to LNCaP treatment. **c**) Comparison of the ratio of CD4 + HLA-DR + regarding the CD4 + . **d**) Comparison of ratio of CD8 + HLA-DR + in regard to the CD8 + . Data analysed by one-way ANOVA and presented as mean bars (n = 10) ± SEM, the significant *p*-value is reported; * indicates $p < 0.05$; n.s. = not significant.

CD4 + or CD8 + cells in untreated samples compared with PBMCs treated with PC-3 EVs, LNCaP EVs and DU 145-EVs (see Supplementary Fig. 9a-d).

We also compared the PBMCs treated with t-NEPC LNCaP EVs and LNCaP-EVs. As shown in Supplementary Fig. 10, no significative differences were observed when comparing the percentage of activated CD4 + and CD8 + cells (Supplementary Fig. 10 a and c). On other hand, when comparing the ratio of CD4 and CD8 positive cells to the total number of cells we observed a significant different between t-NEPC LNCaP EVs and LNCaP-EVs treated PBMCs (Supplementary Fig. 10 b and d; $p < 0.001$ and $p < 0.01$ respectively). Subsequently, we analysed the effect of tNEPC LNCaP-EVs in comparison with PC3 EVs treated PBMCs where no significant changes were detected in the percentages of activated CD4 + cells (Fig. 4a) and CD8 + cells (Fig. 4b) compared to PC-3-EVs treated cells. Then, although no relevant differences were highlighted considering the ratio of activated CD4 cells to total number of cells (Fig. 4c), a statistically significant variation ($p < 0.05$) was observed when comparing tNEPC LNCaP-EVs related ratio for activated CD8 to total cells compared to PC-3-EVs treated cells (Fig. 4d).

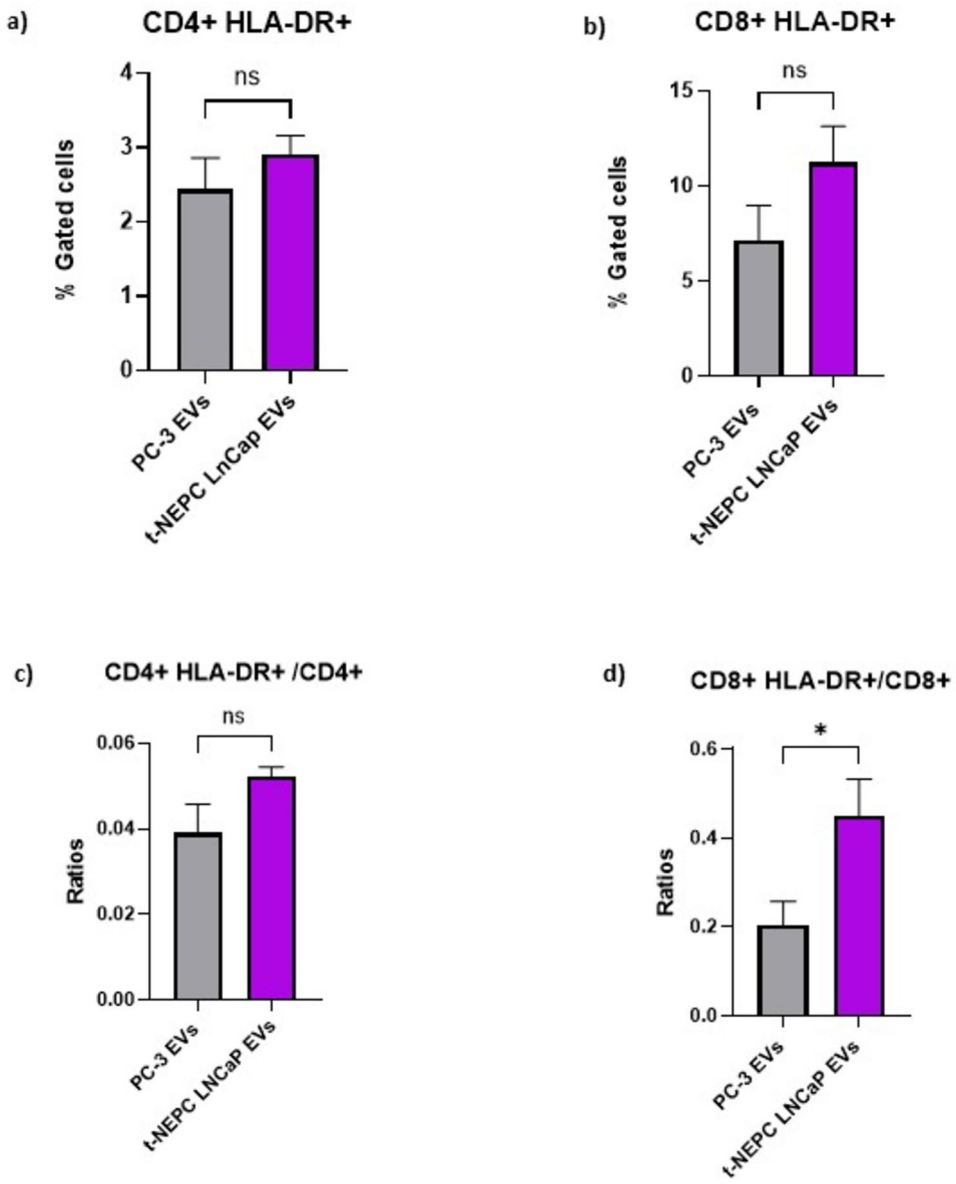

Fig. 4. T-NEPC LNCaP EVs effects on innate lymphoid and NK cells. Effect of t-NEPC LNCaP EVs on innate immune cells. **a**) The percentage of CD4 + HLA-DR + after treatment with EVs derived from PC-3 compared to t-NEPC LNCaP treatment. **b**) The percentage of CD8 + HLA-DR + treated with EVs derived from PC-3 compared to t-NEPC LNCaP treatment. **c**) Comparison of the ratio of CD4 + HLA-DR + regarding the CD4 + . **d**) Comparison of ratio of CD8 + HLA-DR + in regard to the CD8 + . Data analysed by parametric t-test and presented as mean bars (n = 10) ± SEM, the significant *p*-value is reported; * indicates $p < 0.05$; n.s. = not significant.

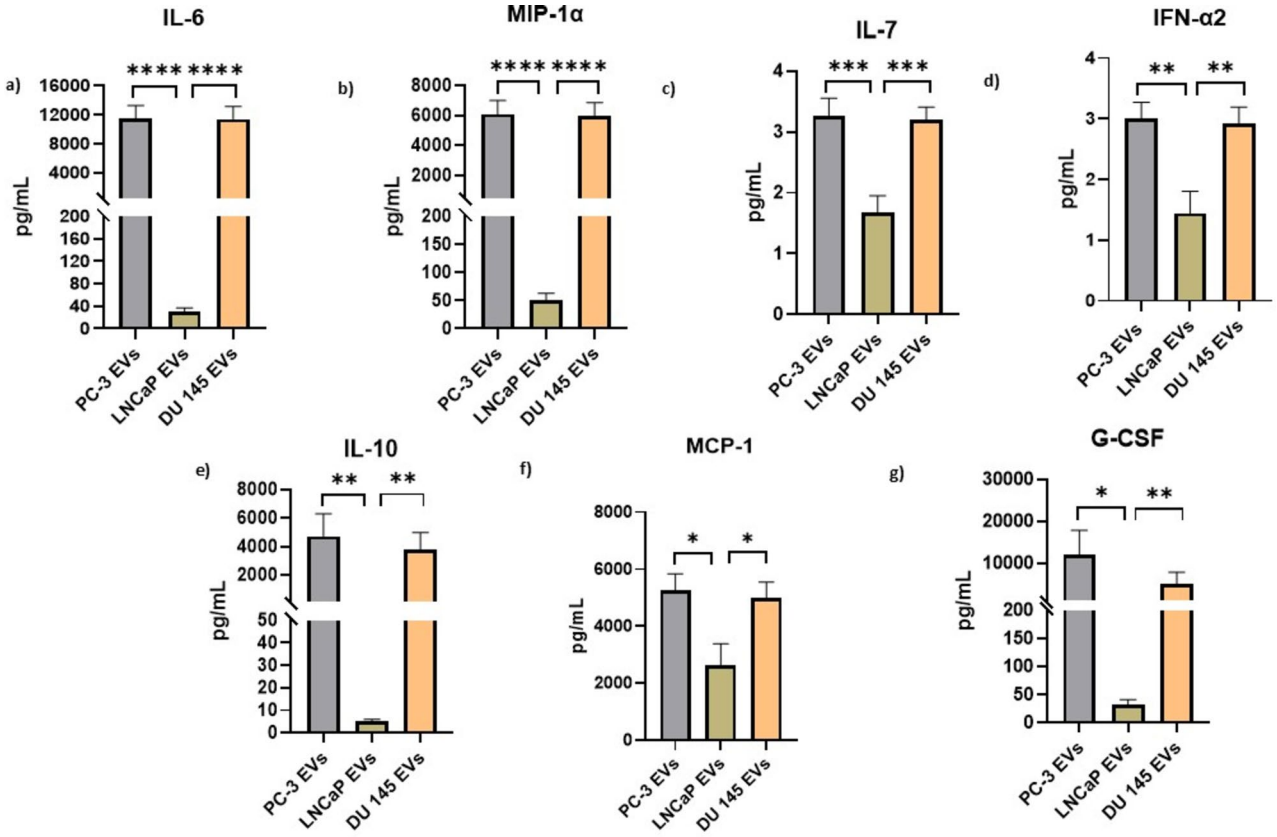

Fig. 5. Release of cytokines by immune cells after treatment with prostate cancer EVs. Seven pro- and anti-inflammatory cytokines were evaluated from the conditioned medium of PBMCs from 10 healthy donors and samples treated with PC-3-EVs, LNCaP-EVs and DU 145 EVs for 24h. **a**) Level of IL-6 between PBMCs treated with PC-3 EVs and DU 145 EVs compared to LNCaP EVs. **b**) Level of MIP-1α between PBMCs treated with PC-3 EVs and DU 145 EVs compared to LNCaP EVs. **c**) Level of IL-7 between PBMCs treated with PC-3 EVs and DU 145 EVs compared to LNCaP EVs. **d**) Level of IFN-α2 between PBMCs treated with PC-3 EVs and DU 145 EVs compared to LNCaP EVs. **e**) Level of IL-10 between PBMCs treated with PC-3 EVs and DU 145 EVs compared to LNCaP EVs. **f**) Level of MCP-1 between PBMCs treated with PC-3 EVs and DU 145 EVs compared to LNCaP EVs. **g**) Level of G-CSF between PBMCs treated with PC-3 EVs and DU 145 EVs compared to LNCaP EVs. Data analysed by one-way ANOVA and presented as mean bars (n = 10) ± SEM, the significant *p*-value is reported; **** indicates $p < 0.0001$; ***indicates $p < 0.001$; ** indicates $p < 0.01$; *indicates $p < 0.05$.

Release of cytokines by immune cells after treatment with prostate cancer EVs

To further investigate the downstream effects of prostate cancer EVs on PBMCs, we evaluated the stimulation of PBMCs by PC-3 EVs, LNCaP EVs and DU 145 EVs in terms of cytokines/interleukins (ILs) released after EVs treatment. Specifically, 13 pro- and anti-inflammatory cytokines were evaluated from conditioned medium of ten PBMCs from healthy donors and samples treated with PC-3 EVs, LNCaP EVs and DU 145 EVs for 24 h (Fig. 5). As illustrated, interleukin-6 (Fig. 5a), MIP- 1α (Fig. 5b), and interleukin-7 (Fig. 5c) levels were significantly ($p < 0.0001$ or $p < 0.001$) higher in the PC-3 and DU 145-EVs treated PBMCs compared to LNCaP EVs treated cells. Likewise, IFN-α2 (Fig. 5d), interleukin-10 (Fig. 5e), MCP-1 (Fig. 5f), and G-CSF (Fig. 5g) showed the same trend with lower significance levels ($p < 0.01$, or $p < 0.05$) for both PC-3 EVs and DU 145 EVs comparisons. Nevertheless, no significant differences were detected for the other eight cytokines/ILs analyzed (Supplementary Fig. 11).

Discussion

The tumor microenvironment is a complex ecosystem where immune cells interact with cancer cells, shaping tumor progression and influencing diagnostic and therapeutic outcomes[32]. EVs are critical mediators of communication within the TME, influencing cancer progression, immune regulation, and resistance to therapy[33]. Tumor-derived EVs, including exosomes and microvesicles, are small membrane-bound vesicles secreted by cancer cells that carry bioactive molecules such as proteins, lipids, nucleic acids, and metabolites[34]. By transferring these molecular cargoes to surrounding cells, tumor EVs modulate various components of the TME, including immune, stromal, and endothelial cells, ultimately shaping tumor growth and metastasis[34,35]. One of the key roles of tumor-derived EVs in the TME is immune modulation. Tumor EVs can suppress

antitumor immunity by directly interfering with immune cell function[36]. For instance, EVs from aggressive tumor cells frequently contain immune checkpoint molecules, such as PD-L1, which can bind to PD-1 receptors on T cells and induce T cell exhaustion, preventing an effective immune response[37]. Additionally, tumor EVs often carry immunosuppressive cytokines, such as TGF-β and IL-10, further dampening immune activation and promoting an immunosuppressive TME[34,38]. Overall, the immune landscape of the TME is highly dynamic and plays a pivotal role in determining tumor fate. Understanding how immune cells interact with cancer cells is crucial for the development of effective diagnostic and therapeutic approaches. The findings of this preliminary study highlight significant differences in the effects of EVs derived from DU 145, PC-3 cells and LNCaP cells on immune cell populations. Our results demonstrate that DU 145 and PC-3 EVs induce an immunomodulatory response compared to LNCaP EVs, with PC-3 exerting the most profound effects and suggesting a potential role for EVs in prostate cancer progression and immune system evasion. Given that the differential metastatic potential of the three cell lines, with LNCaP being lowly metastatic, DU 145 moderately metastatic and PC-3 highly metastatic[12] pairs well with the observed increasing establishment of an immunosuppressive environment in the bloodstream, these findings underscore the importance of immune cells as biomarkers of disease progression and aggressiveness in prostate cancer. The immunomodulatory effects of prostate cancer EVs are evident in their impact on monocyte populations. Specifically, DU 145 EVs and PC-3 EVs significantly reduce the percentage of CD14 + CD16 + monocytes, a subset known to play critical roles in inflammatory responses[39,40]. This suggests that DU 145 EVs and PC-3 EVs may alter the immune landscape by depleting or modulating this monocyte population, potentially contributing to an immunosuppressive tumor microenvironment[41]. In contrast, LNCaP EVs did not elicit the same response, further indicating that EVs from intermediate to highly aggressive cancer cells have distinct immunomodulatory properties. Furthermore, the activation of T cell subsets was clearly distinguished between PC-3 EVs and LNCaP EVs or DU 145 EVs treated immune cells. The significant increase in CD4 + HLA-DR + and CD8 + HLA-DR + cells following treatment with PC-3 EVs, which is, among the three cell lines taken into consideration, the most aggressive one, suggests an enhanced immune activation response, which might be associated with increased antigen presentation or EVs-mediated signalling pathways that stimulate T-cell responses. Given that, HLA-DR expression on CD4 + and CD8 + cells is associated with immune activation in various cancers, this finding underscores the potential utility of these immune markers as indicators of prostate cancer progression[42]. The lack of significant activation in DU 145 EVs and LNCaP EVs treated PBMCs reinforces the concept that higher grade aggressive prostate cancer EVs exert a more profound impact on immune cell dynamics.

Since most of the results were evident when treating PBMCs with EVs derived from androgen unresponsive cell lines compared to AR-dependent LNCaP cells, we also sought whether a direct involvement of AR signaling may be associated to this immunophenotypical switch[43]. Treatment of PBMCs with EVs derived from neuroendocrine transdifferentiated LNCaP cells, which can be considered as a completely different cell line in terms of behaviour, aggressiveness and activated molecular pathways[44]caused a strong suppression of monocyte populations in all treated samples. Although, this mechanism requires further investigation, the phenomenon could be ascribed to the establishment of a particularly strong immunosuppressive milieu[45]. In fact, current research showed several differences in spatial gene expression between NEPC and androgen receptor prostate carcinoma (ARPC) and their gene expression in the TME underling that NEPC is the most lethal prostate cancer, characterized by resistance to hormone therapy, rapid progression, and visceral metastases[46]. The higher ratio of activated CD8 + population in PBMCs treated with tNEPC LNCaP EVs compared with PC-3 EVs further support the aggressiveness of EVs derived from LNCaP tNEPC . Taken all together, these findings did not show a clear pattern of EVs-mediated immune modulation that could be ascribed to differential androgen responsiveness of which additional studies are warranted.

To deepen our analysis, cytokines ELISA on conditioned medium revealed a distinct profile in response to DU 145 EVs and PC-3 EVs rather than LNCaP EVs, which further supports their role in immune modulation[41]. The significantly higher levels of IL-6, MCP-1, IFN-α2, IL-7, MIP-1α, and IL-10 in PC-3 EVs-and DU 145 EVs treated samples suggest a pro-inflammatory and immunosuppressive environment. Elevated IL-6 levels have been linked to cancer progression and poor prognosis[47], while MCP-1 and MIP-1α contribute to monocyte recruitment and chronic inflammation, both of which are critical in shaping the tumor microenvironment[48–50]. The increased presence of IL-10, an immunosuppressive cytokine, further supports the hypothesis that PC-3 and DU 145 EVs may promote immune evasion mechanisms[51,52]. Moreover, IL-7 is a potent pro-inflammatory cytokine known for its ability to destabilize chromosomes and promote tumorigenesis. It plays a dual role in cancer by not only contributing to genomic instability but also influencing tumor growth and progression through the tumor microenvironment and immune system[45]. IL-7 can regulate malignant proliferation by modulating immune responses, enhancing cell survival, and altering the interactions between tumor cells and surrounding tissues[53]. Similarly, G-CSF has tumor-promoting effects on both tumor cells and the tumor microenvironment. Furthermore, high levels of G-CSF are associated with aggressive tumors, which are more difficult to treat and have high mortality rates[54]. In contrast, LNCaP EVs treatment indicate a reduced immunomodulatory effect, suggesting a less aggressive cancer. Indeed, the differential immune responses and their ability to alter monocyte subsets provide insights into how prostate cancer-derived EVs contribute to immune dysregulation, which may have implications for future therapeutic strategies targeting EVs mediated immune interactions. Overall, here we highlight the potential of immune cell populations and their capacities of activation as biomarkers for the progression of prostate cancer. However, a limitation of the study is the effect of prostate cancer EVs analysed solely on healthy derived PBMCs. Future studies will be extended on the validation on patient derived PBMCs, while high-throughput analysis of EVs cargo will help to correlate the clinical stage of each patient. Additionally, further investigation on profiling EVs content relevant to immune landscape will serve as a valuable tool for assessing tumor aggressiveness and patient prognosis.

Conclusion

Our study provides preliminary evidence that prostate cancer EVs exert distinct immunomodulatory effects depending on their cellular origin. Particularly, the differences observed between PC-3 EVs, LNCaP EVs, DU 145 EVs, and tNEPC LNCaP EVs highlight the potential use of immune cell markers as reliable indicators of disease progression. Further studies are warranted to fully elucidate the network between prostate cancer EVs and immune cells. However, these findings into the specific mechanisms by which EVs mediate immune modulation could pave the way for novel diagnostic and therapeutic approaches in prostate cancer management.

Material and methods

Cell lines

The androgen-dependent LNCaP metastatic prostate carcinoma cell line (CRL-1740), androgen-independent prostate carcinoma PC-3 cell line (CRL-1435) and androgen-independent prostate carcinoma DU 145 cell line (HTB-81) were purchased from the American Type Culture Collection (ATCC). LNCaP and DU 145 cells were maintained in Roswell Park Memorial Institute (RPMI) 1640 medium (Gibco – Fisher Scientific) supplemented with 10% FBS (GE Healthcare), 1 × Pen-Strep (Lonza), and 2 mM l-glutamine (Lonza). PC-3 cells were maintained in Dulbecco's Modified Eagle's medium/nutrient mixture F-12 (DMEM/F-12) (Gibco – Fisher Scientific) supplemented with 10% FBS (GE Healthcare), 1 × Pen-Strep (Lonza), and 2 mM l-glutamine (Lonza). Cells were maintained in a humidified incubator at 37 °C in the presence of 5% CO2, and all experiments were performed under exponential growth conditions. Cells were authenticated by STR and periodically tested for mycoplasma contamination using a MycoBlue Mycoplasma Detector D101 (cat: D101-01; Vazyme Biotech). For LNCaP neuroendocrine transdifferentiation, LNCaP cells were cultivated for 18 days in Roswell Park Memorial Institute (RPMI) 1640 medium w/o phenol red (Gibco – Fisher Scientific) supplemented with 10% dextran coated charcoal stripped FBS (GE Healthcare), 1 × Pen-Strep (Lonza), and 2 mM l-glutamine (Lonza), following our previous publication[55] .

Separation of EVs from prostate cancer cells

EVs derived from PC-3, LNCaP, DU 145 and tNEPC LNCaP cell lines were separated using differential ultracentrifugation as previously described[57]. Before EVs separation, all cell models were cultured in exo-free medium for 48 h (w/o phenol red in the case of tNEPC LNCaP), and the medium was centrifuged twice (300xg and then 2000xg) for 10 min to remove dead cells and debris. Next, larger EVs and remaining cell debris were removed by ultracentrifugation at 10,000 × g for 30 min at 4 °C using OPTIMA MAX-XP (Cat: # 393,315, Beckman Coulter, Brea, CA, USA). The conditioned medium was subjected to ultracentrifugation at 200,000 × g for 70 min at 4 °C to pellet EVs. EVs pellets were subsequently washed using 0.22 µm filtered PBS at 200,000 × g for 70 min. Finally, the enriched EVs samples were resuspended in 200 µL of 0.22 µm filtered PBS and used immediately for further analysis.

Analysis of particle concentration and size using nanoparticle tracking analysis (NTA)

Prostate EVs samples were analyzed using NanoSight NS300 (Malvern Instruments Ltd., Malvern, UK). Specifically, the EVs samples were injected into the NTA system under constant flow conditions (flow rate = 50). Five × 60 s videos were recorded and analyzed using NTA 3.2 software (Malvern Instruments Ltd., Malvern, UK). Three biological replicates of each sample were independently analyzed using NanoSight NS300.

Immunoblotting analysis of EVs and neuroendocrine markers

Prostate EVs samples were analyzed by immunoblotting as described previously[56]. Lysed EVs were resolved on 10% Mini-PROTEAN® TGX Stain-Free™ (Bio-Rad Laboratories, Hercules, CA, USA, Cat. #4,568,034) at 120 V, and proteins were transferred by the Trans-Blot Turbo System (Bio-Rad Laboratories, Cat. # 690BR024275). The filters were blocked with 5% milk in TBST containing 0.1% Tween-20 for 1 h and incubated overnight at 4 °C with primary antibodies. Specifically, anti-calnexin (1:1000; Cat. # ab10286; Abcam, Cambridge, UK), anti-syntenin (1:1000; Cat. # ab19903, Abcam, Cambridge, UK), and anti-CD63 (1:1000; Cat. #ab68418, Abcam, Cambridge, UK). The secondary antibodies used were Goat Anti-Mouse IgG (1:2000; Cat. # 10,303–05, Biotech, Alpharetta, GA, USA) or Goat Anti-Rabbit IgG (1:2000; Cat. # 4030–05, Biotech), and the filters were incubated for 1 h at RT. Imaging was performed using an automated ChemiDoc™ MP Imaging System (Bio-Rad Laboratories, Cat. # 12,003,154, Segrate, MI, Italy) and Clarity Max™ Western ECL Substrate (Cat. # 1,705,062, Bio-Rad Laboratories, Segrate, MI, Italy). PC-3 and LNCaP cell lysates (CL) were used as positive controls. To confirm neuroendocrine transdifferentiation, total cell lysates from LNCaP and tNEPC LNCaP samples were analysed by Immunoblotting as previously described. After milk blocking, the following primary antibodies were incubated: anti-NSE (1:1000; Cat. #ab218388, Abcam, Cambridge, UK), anti-CHGA (1:1000, Cat. #ab283265, Abcam, Cambridge, UK) and anti-vinculin (1:2000, Cat. #V9131, Sigma-Aldrich).

Scanning electron microscopy of prostate cancer EVs

EVs morphology was analyzed by scanning electron microscopy (SEM). EVs derived from PC-3, LNCaP and DU 145 cell lines were prepared as previously described[58]. After ultracentrifugation, the EVs pellets were suspended in 2% paraformaldehyde (PFA) and incubated at 4 °C overnight. Next, samples in PFA were ultracentrifuged at 100,000xg for 2 h and the EVs pellets were resuspended in 200 µL of deionized H_2O. Finally, the fixed samples were dried overnight under a vacuum pump and directly coated with gold (7 nm thick) before imaging. Gold-coated EVs samples were examined using a PHENOM PROX scanning electron microscope (Thermo Fisher).

Peripheral blood mononuclear cell (PBMCs) isolation and EVs treatment

PBMCs were obtained from ten healthy men from a cohort of healthy subjects enrolled for this study, in accordance with the Declaration of Helsinki and approved by the Ethics Committee of IRCCS PASCALE, Naples, Italy (CET Campania1 of Naples, Italy; reference number 4/23, 2023). Informed consent was obtained from all subjects involved in the study. PBMCs were recovered from venous blood using density gradient centrifugation (PAN-Biotech, cat: P04-6050). Briefly, each blood sample was diluted 1:5 in PBS (Gibco) and slowly transferred to a 15 mL conical tube containing 3 mL of Pancoll, ensuring that the different phases remained separated. The tubes were centrifuged at 1500 rpm for 20 min at room temperature (RT), and the interphases with white rings containing PBMCs were carefully isolated and transferred into a new tube containing 8 mL of PBS for washing by centrifugation at 1300 rpm for 5 min at RT. PBMCs pellets were subsequently resuspended in 8 mL of Erythrocyte Lysis Buffer 1x (PAN-Biotech, cat: P10-90,100) and incubated for 10 min at RT on a vertical rotating wheel to deplete any residual erythrocyte contaminants. Cells were centrifuged at 1300 rpm for 5 min at RT, and the pellets were resuspended in complete RPMI 1640 medium. PBMCs were counted and aliquoted at 500,000 viable cells/100µL RPMI medium in multiple 1.5 mL tubes for PBCMs + EVs incubation. The experimental conditions were as follows: a) control (CTRL) samples + 10µL µL PBS; b) PBMCs + LNCaP-derived EVs samples, 10µL of resuspended LNCaP EVs, equivalent to 10^8 EVs; c) PBMCs + PC-3-derived EVs samples, 10µL of resuspended PC-3 EVs, equivalent to 10^8 EVs; d) PBMCs + DU 145-derived EVs samples, 10µL of resuspended DU 145 EVs, equivalent to 10^8 EVs; e) PBMCs + tNEPC LNCaP-derived EVs samples, 10µL of resuspended tNEPC LNCaP EVs, equivalent to 10^8 EVs. The tubes were maintained in a humidified incubator at 37 °C in the presence of 5% CO2. After 6 h, 50 µL of the cell suspension was collected from each tube and processed for monocyte population analysis. After 24 h, the remaining cell suspension was collected from each tube, centrifuged at 4000 rpm for 5 min at RT, and the resulting cell pellet was processed for innate and adaptive immunity population analysis. The supernatant medium was stored at -80 °C for the detection of cytokines.

Immune populations screening using flow cytometry analysis

Treated (PC-3 EVs, LNCaP, DU 145 and tNEPC LNCaP EVs) and untreated PBMCs were analyzed using a CytoFLEX flow cytometer (Beckman Coulter, Brea, CA, USA). Surface marker detection was performed by staining PBMCs with the following antibodies: CD169-PE, PD-1-PC7, HLA-DR-APC, CD14-APC700, CD16-APC750, CD64-PB450, and CD45-KO525 for monocyte identification, and CD31-FITC, CD335-PE, HLA-DR-ECD, CD337-PC5, CD3-PC7, CD56-APC, CD71-APC700, CD7-APC750, CD4-PB540, and CD45-KO525 for other immune components. Each antibody was prepared at a 1:10 dilution and thoroughly mixed. All the antibodies were purchased from Beckman Coulter. Immune cells analysis was performed using the Kaluza 2.1 software (Beckman Coulter, USA).

Secreted inflammatory cytokines analysed by ELISA

After 24 h of incubation, the media from the treated (PC-3 EVs, LNCaP EVs and DU 145 EVs) and untreated PBMCs were collected for cytokine quantification. Specifically, the LEGENDplex™ COVID-19 Cytokine Storm Panel 1 (cat. #741,091, BioLegend, San Diego, USA) was used to detect IL-6, MCP-1, G-CSF, IFN-α2, IL-2, IFN-γ, IL-7, IL-1RA, CXCL8, TNF-α, CXCL10 (IP-10), MIP-1α, and IL-10, according to the manufacturer's instructions.

Statistical analysis

P-values were calculated using GraphPad Prism 10 (GraphPad Software), as described in the individual figure legends, and were considered significant if $p < 0.05$. Statistical differences were calculated using parametric t-tests, multiple parametric t-tests, and one-way ANOVA test. The sample size was not predetermined using statistical methods, and the experiments were not randomized. Data reported in this study were obtained in triplicate and are presented as mean ± SEM.

We have submitted all relevant data of our experiments to the EV-TRACK knowledgebase (EV-TRACK ID: EV250049).

Data availability

Data available on request from the authors. All relevant data regarding PCa EVs experiments are available in a public repository the EV-TRACK knowledgebase (EV-TRACK ID: EV250049) via the following URL: http://evtrack.org/review.php. Please use the EV-TRACK ID (EV250049) and the last name of the first author (Pecoraro) to access our data depository. The data that support the findings of this study are available on request from the corresponding author, J.S.

Received: 18 July 2025; Accepted: 5 December 2025
Published online: 10 December 2025

References

1. Bray, F. et al. Global cancer statistics 2022: GLOBOCAN estimates of incidence and mortality worldwide for 36 cancers in 185 countries. *Cancer J. Clin.* **74**, 229–263 (2024).
2. Ferlay, J. et al. Cancer incidence and mortality worldwide: Sources, methods and major patterns in GLOBOCAN 2012. *Int. J. Cancer* **136**, E359–E386 (2015).
3. Humphrey, P. A. Histopathology of Prostate Cancer. *Cold Spring. Harb. Perspect. Med.* **7**, a030411 (2017).
4. Sun, C. et al. Modified the 8th AJCC staging system for patients with advanced prostate cancer: a study based on SEER database. *BMC Urol.* **22**, 185 (2022).

5. Van Poppel, H. et al. Serum PSA-based early detection of prostate cancer in Europe and globally: past, present and future. *Nat. Rev. Urol.* **19**, 562–572 (2022).
6. Ge, Q. et al. Molecular classifications of prostate cancer: basis for individualized risk stratification and precision therapy. *Ann. Med.* **55**, 2279235 (2023).
7. Gillessen, S. et al. Management of patients with advanced prostate cancer. Part I: intermediate-/high-risk and locally advanced disease, biochemical relapse, and side effects of hormonal treatment: report of the advanced prostate cancer consensus conference 2022. *Eur. Urol.* **83**, 267–293 (2023).
8. Sandhu, S. et al. Prostate cancer. *Lancet* **398**, 1075–1090 (2021).
9. Horoszewicz, J. S. et al. The LNCaP cell line–a new model for studies on human prostatic carcinoma. *Prog. Clin. Biol. Res.* **37**, 115–132 (1980).
10. Stone, K. R., Mickey, D. D., Wunderli, H., Mickey, G. H. & Paulson, D. F. Isolation of a human prostate carcinoma cell line (DU 145). *Int. J. Cancer* **21**, 274–281 (1978).
11. Kaighn, M. E., Narayan, K. S., Ohnuki, Y., Lechner, J. F. & Jones, L. W. Establishment and characterization of a human prostatic carcinoma cell line (PC-3). *Invest. Urol.* **17**, 16–23 (1979).
12. Molter, C. W. et al. Prostate cancer cells of increasing metastatic potential exhibit diverse contractile forces, cell stiffness, and motility in a microenvironment stiffness-dependent manner. *Front. Cell Dev. Biol.* **10**, 932510 (2022).
13. Namekawa, T., Ikeda, K., Horie-Inoue, K. & Inoue, S. Application of prostate cancer models for preclinical study: advantages and limitations of cell lines, patient-derived Xenografts, and three-dimensional culture of patient-derived cells. *Cells* **8**, 74 (2019).
14. Kozlowski, J. M. et al. Metastatic behavior of human tumor cell lines grown in the nude mouse. *Cancer Res.* **44**, 3522–3529 (1984).
15. Hinshaw, D. C. & Shevde, L. A. The Tumor Microenvironment Innately Modulates Cancer Progression. *Cancer Res.* **79**, 4557–4566 (2019).
16. Kaur, H. B. et al. Association of tumor-infiltrating T-cell density with molecular subtype, racial ancestry and clinical outcomes in prostate cancer. *Mod. Pathol.* **31**, 1539–1552 (2018).
17. Petitprez, F. et al. PD-L1 Expression and CD8+ T-cell Infiltrate are Associated with Clinical Progression in Patients with Node-positive Prostate Cancer. *Eur. Urol. Focus* **5**, 192–196 (2019).
18. Woo, J. R. et al. Tumor infiltrating B-cells are increased in prostate cancer tissue. *J. Transl. Med.* **12**, 30 (2014).
19. Ammirante, M., Luo, J.-L., Grivennikov, S., Nedospasov, S. & Karin, M. B-cell-derived lymphotoxin promotes castration-resistant prostate cancer. *Nature* **464**, 302–305 (2010).
20. Teijeira, A. et al. Metabolic Consequences of T-cell Costimulation in Anticancer Immunity. *Cancer Immunol. Res.* **7**, 1564–1569 (2019).
21. Lu, X. et al. Effective combinatorial immunotherapy for castration-resistant prostate cancer. *Nature* **543**, 728–732 (2017).
22. Altuna-Coy, A., Ruiz-Plazas, X., Arreaza-Gil, V., Segarra-Tomás, J. & Chacón, M. R. In silico analysis of prognostic and diagnostic significance of target genes from prostate cancer cell lines derived exomicroRNAs. *Cancer Cell Int.* **23**, 275 (2023).
23. Skotland, T., Hessvik, N. P., Sandvig, K. & Llorente, A. Exosomal lipid composition and the role of ether lipids and phosphoinositides in exosome biology. *J. Lipid Res.* **60**, 9–18 (2019).
24. Valadi, H. et al. Exosome-mediated transfer of mRNAs and microRNAs is a novel mechanism of genetic exchange between cells. *Nat. Cell Biol.* **9**, 654–659 (2007).
25. Naito, Y., Yoshioka, Y., Yamamoto, Y. & Ochiya, T. How cancer cells dictate their microenvironment: present roles of extracellular vesicles. *Cell Mol. Life Sci.* **74**, 697–713 (2017).
26. Ramteke, A. et al. Exosomes secreted under hypoxia enhance invasiveness and stemness of prostate cancer cells by targeting adherens junction molecules. *Mol. Carcinog.* **54**, 554–565 (2015).
27. Deep, G. et al. Exosomes secreted by prostate cancer cells under hypoxia promote matrix metalloproteinases activity at pre-metastatic niches. *Mol. Carcinog.* **59**, 323–332 (2020).
28. Guo, Y. et al. Effects of exosomes on pre-metastatic niche formation in tumors. *Mol. Cancer* **18**, 39 (2019).
29. Li, I. & Nabet, B. Y. Exosomes in the tumor microenvironment as mediators of cancer therapy resistance. *Mol. Cancer* **18**, 32 (2019).
30. Mashouri, L. et al. Exosomes: composition, biogenesis, and mechanisms in cancer metastasis and drug resistance. *Mol. Cancer* **18**, 75 (2019).
31. Welsh, J. A. et al. Minimal information for studies of extracellular vesicles (MISEV2023): From basic to advanced approaches. *J. Extracell. Vesicles* **13**, e12404 (2024).
32. de Visser, K. E. & Joyce, J. A. The evolving tumor microenvironment: From cancer initiation to metastatic outgrowth. *Cancer Cell* **41**, 374–403 (2023).
33. Tao, S.-C. & Guo, S.-C. Role of extracellular vesicles in tumour microenvironment. *Cell Commun. Signal.* **18**, 163 (2020).
34. Kumar, M. A. et al. Extracellular vesicles as tools and targets in therapy for diseases. *Sig. Transduct. Target Ther.* **9**, 1–41 (2024).
35. Wang, S., Sun, J., Dastgheyb, R. M. & Li, Z. Tumor-derived extracellular vesicles modulate innate immune responses to affect tumor progression. *Front. Immunol.* **13**, 1045624 (2022).
36. Vergani, E. et al. Extracellular vesicles in anti-tumor immunity. *Semin. Cancer Biol.* **86**, 64–79 (2022).
37. Reale, A., Khong, T. & Spencer, A. Extracellular vesicles and their roles in the tumor immune microenvironment. *J. Clin. Med.* **11**, 6892 (2022).
38. Mittal, S., Gupta, P., Chaluvally-Raghavan, P. & Pradeep, S. Emerging role of extracellular vesicles in immune regulation and cancer progression. *Cancers (Basel)* **12**, 3563 (2020).
39. Szaflarska, A. et al. Antitumor response of CD14+/CD16+ monocyte subpopulation. *Exp. Hematol.* **32**, 748–755 (2004).
40. Ziegler-Heitbrock, L. The CD14+ CD16+ blood monocytes: their role in infection and inflammation. *J. Leukoc Biol.* **81**, 584–592 (2007).
41. Novysedlak, R. et al. The immune microenvironment in prostate cancer: a comprehensive review. *Oncology* **103**, 521–545 (2024).
42. Huang, L., Kirschke, C. P. & Zhang, Y. Decreased intracellular zinc in human tumorigenic prostate epithelial cells: a possible role in prostate cancer progression. *Cancer Cell Int.* **6**, 10 (2006).
43. Sargos, P. et al. Characterization of prostate neuroendocrine cancers and therapeutic management: a literature review. *Prostate Cancer Prostatic Dis.* **17**, 220–226 (2014).
44. Yuan, T.-C. et al. Androgen deprivation induces human prostate epithelial neuroendocrine differentiation of androgen-sensitive LNCaP cells. *Endocr. Relat. Cancer* **13**, 151–167 (2006).
45. Brady, L. & Nelson, P. S. RISING STARS: Heterogeneity and the tumor microenvironment in neuroendocrine prostate cancer. *J. Endocrinol.* https://doi.org/10.1530/JOE-22-0211 (2023).
46. Watanabe, R. et al. Spatial Gene Expression Analysis Reveals Characteristic Gene Expression Patterns of De Novo Neuroendocrine Prostate Cancer Coexisting with Androgen Receptor Pathway Prostate Cancer. *Int. J. Mol. Sci.* **24**, 8955 (2023).
47. Mitsui, E. et al. Novel treatment strategy targeting interleukin-6 induced by cancer associated fibroblasts for peritoneal metastasis of gastric cancer. *Sci. Rep.* **15**, 3267 (2025).
48. Zhao, H. et al. Inflammation and tumor progression: signaling pathways and targeted intervention. *Sig. Transduct Target Ther.* **6**, 1–46 (2021).
49. Galland, S., Martin, P., Fregni, G., Letovanec, I. & Stamenkovic, I. Attenuation of the pro-inflammatory signature of lung cancer-derived mesenchymal stromal cells by statins. *Cancer Lett.* **484**, 50–64 (2020).

50. Mempel, T. R., Lill, J. K. & Altenburger, L. M. How chemokines organize the tumour microenvironment. *Nat. Rev. Cancer* **24**, 28–50 (2024).
51. Carlini, V. et al. The multifaceted nature of IL-10: regulation, role in immunological homeostasis and its relevance to cancer, COVID-19 and post-COVID conditions. *Front. Immunol.* **14**, 1161067 (2023).
52. Rojas, J. M., Avia, M., Martín, V. & Sevilla, N. IL-10: A Multifunctional Cytokine in Viral Infections. *J. Immunol. Res.* **2017**, 6104054 (2017).
53. Lin, J. et al. The role of IL-7 in Immunity and Cancer. *Anticancer Res.* **37**, 963–967 (2017).
54. Ioannis, K., Eralda, S., Egal, E. S. A. & Beswick, E. G-CSF in tumors: aggressiveness, tumor microenvironment and immune cell regulation. *Cytokine* **142**, 155479 (2021).
55. Pecoraro, G. et al. Co-modulation of a circular form of PCDH11Y during neuroendocrine differentiation of prostate cancer. *Front. Oncol.* **15**, 1502405 (2025).
56. Leone, I. et al. Triple-Negative Breast Cancer EVs Modulate Growth and Migration of Normal Epithelial Lung Cells. *Int. J. Mol. Sci.* **25**, 5864 (2024).
57. Santoro, J. et al. Influence of Breast Cancer Extracellular Vesicles on Immune Cell Activation: A Pilot Study. *Biology* **12**, 1531 (2023).
58. Zhang, H., Silva, A. C., Zhang, W., Rutigliano, H. & Zhou, A. Raman Spectroscopy characterization extracellular vesicles from bovine placenta and peripheral blood mononuclear cells. *PLoS ONE* **15**, e0235214 (2020).
59. Van Deun, J. et al. EV-TRACK: transparent reporting and centralizing knowledge in extracellular vesicle research. *Nat. Methods* **14**, 228–232 (2017).

Acknowledgements
The authors would like to thank SDN Biobank, partner of BBMRI.it, the Italian node of BBMRI-ERIC (Biobanking and BioMolecular Research Infrastructure—European Research Infrastructure Consortium).

Author contributions
J.S., G.P. performed conception and design. J.S., G.S. performed analysis and data acquisition. J.S, G.S. made intellectual contributions to the study design and review of data. J.S., G.P., G.S., wrote, reviewed, and revised the manuscript.

Funding
This work was founded by the "Progetto di Ricerca Corrente" of the Italian Ministry of Health.

Declarations

Competing interests
The authors declare no competing interests.

Additional information
Supplementary Information The online version contains supplementary material available at https://doi.org/10.1038/s41598-025-31838-w.

Correspondence and requests for materials should be addressed to J.S.